Dynamical Climatology

The effect of a shoaling thermocline on equatorially-trapped Kelvin waves.

by

A.E. Gill and B.A. King

DCTN 27 August 1985

Meteorological Office (Met. O. 20)
London Road
Bracknell
Berkshire RG12 2SZ

DYNAMICAL CLIMATOLOGY TECHNICAL NOTE NO. 27

THE EFFECT OF A SHOALING THERMOCLINE ON EQUATORIALLY-TRAPPED KELVIN WAVES

by

A E Gill

Met Office Unit, Hooke Institute, Clarendon Lab., Oxford

and

B A King

Institute of Oceanographic Sciences, Wormley, Godalming, Surrey

Submitted for publication to the Journal of Physical Oceanography

Met O 20 (Dynamical
Climatology Branch)
Meteorological Office
London Road
Bracknell
Berkshire, U.K. RG12 2SZ

August 1985

Note: This paper has not been published. Permission to quote from it should be obtained from the Assistant Director of the above Meteorological Office Branch.

Abstract

The effect of the sloping thermocline in the equatorial Pacific on Kelvin wave propagation is examined by means of a model with two active layers. High-frequency waves, which include those of two to three weeks period, conform to WKBJ theory and there is very little energy transfer between vertical modes. Low-frequency perturbations, on the other hand, such as those associated with El Nino events, experience significant energy transfer between modes. The amount of transfer increases as the frequency decreases until a limit is reached where the shoaling part of the thermocline acts like a step. Thus it is possible that second baroclinic mode perturbations observed in the eastern Pacific occur as a result of transfer of energy from remotely forced first baroclinic mode Kelvin waves.

1. Introduction

Considerable variability in the eastern equatorial Pacific results from perturbations arriving from the west in the form of equatorially-trapped Kelvin waves. The role of these waves in raising sea-level and depressing the thermocline on the eastern boundary during El Nino conditions has been amply demonstrated by models (see Gill 1982a). Observations at different points on the equator (Knox and Halpern 1982, Eriksen et al. 1983) are consistent with signals being propagated eastwards at a speed close to that of the Kelvin wave associated with the first vertical mode. In fact the evidence suggested a slightly faster speed which was attributed to the effect of mean currents. The perturbations in these cases have periods of order two or three weeks.

From the above, one might be tempted to conclude that the first vertical mode is dominant in the equatorial Pacific, but investigations of vertical structure show that other modes are important as well. Gill (1982b) looked at bathythermograph records on the equator during 1971-73 and found cases where large changes in vertical structure occurred over two or three months. The variation of isotherm displacement with depth for the central Pacific was consistent with the first mode being dominant, but the variation found for the eastern Pacific was not, being similar to that for the second baroclinic mode.

This result prompted the present study by raising the following question. Suppose a first mode Kelvin wave is generated in the western Pacific. How will it be altered by the changes in mean structure of the ocean as it propagates eastwards? In particular, is it possible that it will change to such an extent that the second mode

is dominant by the time the signal reaches the eastern boundary?

Before discussing the model that was developed to address this question, some recent work on vertical structure should also be mentioned. A theoretical study by Gent (1985) of the wind driven annual cycle shows that many modes are needed to describe the observed changes in vertical structure, and the first mode is by no means dominant. His model did not take account of zonal variations in structure and it is possible these may be responsible for some of the difficulties he had in reproducing some features of the observed structure. Also, results of other observational studies of vertical structure are becoming available. In particular, Behringer (1984,1985) and Leetmaa (1985) find the first three or four modes to be important for describing changes in structure in the equatorial eastern Pacific.

This study is not addressed to assessing what the vertical structure might be in any one location, but to investigating whether the modal decomposition of a wave can undergo significant changes as a result of propagation through a region of shoaling thermocline. The starting point, therefore, is to construct the simplest model we can think of which can be used to address this question. Clearly, it must have more than one vertical mode, so we choose a model with two active near-surface layers overlying a deep layer at rest. The interface between the deep water and the second layer is assumed horizontal in the unperturbed state, rather like the 12 isotherm in the Pacific which is at a depth of about 300m in both the east and west (see Fig. 11.17 in Gill 1982a). The interface between the two active layers, on the other hand, shoals toward the east, rather like the 18 isotherm, say, which shoals from around 180m in the central Pacific to around 20m in the east. In equilibrium, the shoaling is maintained by

a wind stress represented as a body force distributed over the uppermost layer.

For simplicity, imagine a semi-infinite region to the west of the shoaling zone where both interfaces are flat. A single mode (first or second) Kelvin wave propagates at uniform speed along this section and then enters the shoaling region where changes in its properties begin to take place. For convenience, the shoaling is supposed uniform, i.e. the interface has a constant slope, and this slope terminates at a definite longitude where the interface again becomes flat. This uniform region can be envisaged to extend indefinitely to the east.

As a background to the equatorial problem, the non-rotating case is first examined. In particular, the nature of two extreme limits is determined. The high-frequency limit corresponds to waves which are very short compared with the length of the shoaling region. For these waves, the change in environment as they propagate seems very slow and they adjust to the changes as they go along. WKBJ theory applies and energy always remains in the same mode. Changes in amplitude can be determined by the condition that the energy flux remains constant.

The low-frequency limit corresponds to waves which are so long that the shoaling appears to take place in no distance at all. In other words, the shoaling region behaves like a step. The mathematical problem, therefore, reduces to applying matching conditions at the step in order to find how much energy is transmitted in each of the two available modes, and how much is reflected. In realistic circumstances, the reflection of energy is not usually important, but the energy transmitted may be distributed between the modes in quite a different way to the incident wave. If two modes are incident, the subdivision between the transmitted modes depends on

whether the incident modes are reinforcing or otherwise when they hit the step.

The results for an equatorial beta-plane and for finite incident pulses are obtained numerically. The high- and low-frequency limiting results conform closely to what one would expect on the basis of the non-rotating theory, and there is a smooth transition in between the two limits. On this basis, it is clear that the long pulses of months or more duration associated with El Nino events see the shoaling thermocline as a step, and so can have quite a different modal structure at the eastern boundary from that which is obtained in the western and central Pacific. Waves with two or three weeks period, on the other hand, have inverse wavenumbers of 6 or 7 degrees of longitude so are much nearer the WKBJ limit and are not severely modified.

The arrangement of the remainder of the paper is as follows. Section 2 gives the model equations and the appropriate non-dimensionalisation. Normal modes and their properties are discussed in Section 3 and the energy equation is described in Section 4. The results for short (high-frequency) waves are obtained in Section 5 both for the non-rotating case and for Kelvin waves. In Section 6, however, the low-frequency (long-wave) limit is calculated only for the non-rotating case. Finally in Section 7 numerical results are obtained for the case of an incident mode 1 Kelvin wave on a shoaling thermocline for pulses of a whole range of lengths which effectively span the transition from the WKBJ limit to the low frequency limit.

2. The model equations

Consider a three-layer ocean as depicted in Fig. 1 with the lower layer at rest. The index i (i = 1,2,3) will be used to denote the i^{th} layer, starting from the top. The thickness of the layer is H_i, its density ρ_i and its horizontal velocity is (u_i, v_i). An equatorial beta-plane will be used with y denoting distance northwards and x distance eastwards (Gill 1982a Chapter 11).

The equations of motion take the form

$$\frac{\partial u_i}{\partial t} - \beta y v_i = -\frac{\partial p_i}{\partial x} + X \qquad (2.1)$$

$$\frac{\partial v_i}{\partial t} + \beta y u_i = -\frac{\partial p_i}{\partial y} \qquad (2.2)$$

$$\frac{\partial H_i}{\partial t} + \frac{\partial}{\partial x}(H_i u_i) + \frac{\partial}{\partial y}(H_i v_i) = 0 \qquad (2.3)$$

where p_i is the pressure divided by density in layer i and $\beta = 2.3 \times 10^{-11}\ m^{-1} s^{-1}$ is the gradient of the Coriolis parameter. The forcing term X appears only in the top layer and represents the effect of wind forcing in that layer. In the present context, the only purpose of this term is to provide the forcing that maintains the slope of the thermocline.

The pressure in each layer can be calculated from hydrostatics (Gill 1982a, Chapter 6) and the assumption of zero pressure gradient in the lower layer used to give p_1 and p_2 in terms of H_1 and H_2. The result is

$$\left.\begin{aligned} p_1 &= g_3 H_1 + g_2 H_2 \\ p_2 &= g_2 H_1 + g_2 H_2 \end{aligned}\right\} \qquad (2.4)$$

where the reduced-gravity coefficients g_i are given by

$$\left.\begin{aligned} g_1 &= (\rho_2 - \rho_1) g / \rho_1 \\ g_2 &= (\rho_3 - \rho_2) g / \rho_1 \\ g_3 &= (\rho_3 - \rho_1) g / \rho_1 = g_1 + g_2 \end{aligned}\right\} \qquad (2.5)$$

and g is the acceleration due to gravity.

Consider now the equilibrium solution, which will consist of two regimes. In one there is no forcing, so H_1 and H_2 are constant. In the other regime, the forcing X in the upper layer is constant and so induces a uniform slope on the upper layer. Combining (2.1), (2.4) and (2.5) with i = 1,2 leads to the result that the combined thickness $H_1 + H_2$ of the two active layers is constant, but H_1 varies according to

$$g_1 \partial H_1 / \partial x = X \qquad (2.6)$$

The next step is to consider small perturbations from the equilibrium, with h_i used to denote the perturbation to H_i. Furthermore a non-dimensional co-ordinate system will be used where $H_1 + H_2$ is the depth scale,

$$c = \left(g_3 (H_1 + H_2)\right)^{1/2} \qquad (2.7)$$

is the velocity scale, and the Rossby radius

$$R = (c/2\beta)^{1/2} \qquad (2.8)$$

is the horizontal length scale. The perturbation equations then take the form

$$\left.\begin{aligned} \frac{\partial u_i}{\partial t} - \tfrac{1}{2} y v_i &= -\frac{\partial p_i}{\partial x} \\ \frac{\partial v_i}{\partial t} + \tfrac{1}{2} y u_i &= -\frac{\partial p_i}{\partial y} \end{aligned}\right\} \quad (2.9)$$

$$\left.\begin{aligned} \frac{\partial h_1}{\partial t} + \frac{\partial}{\partial x}(\phi u_1) + \frac{\partial}{\partial y}(\phi v_1) &= 0 \\ \frac{\partial h_2}{\partial t} + \frac{\partial}{\partial x}((1-\phi) u_2) + \frac{\partial}{\partial y}((1-\phi) v_2) &= 0 \end{aligned}\right\} \quad (2.10)$$

where

$$\left.\begin{aligned} p_1 &= h_1 + r h_2 \\ p_2 &= r(h_1 + h_2) \end{aligned}\right\} \quad (2.11)$$

and

$$\left.\begin{aligned} \phi &= H_1/(H_1+H_2) \\ r &= g_2/g_3 = (\rho_3-\rho_2)/(\rho_3-\rho_1) \end{aligned}\right\} \quad (2.12)$$

are both ratios that are less than unity. The first ratio gives the fraction of the total active depth occupied by the upper layer. In the unforced region it is a constant, whereas in the forced region it has a constant gradient given by

$$d\phi/dx = -\epsilon \quad (2.13)$$

where ϵ is small. The ratio r gives the change in density at the bottom of the second layer as a fraction of the total change over the two layers.

Many of the analytic results will be obtained for the non-rotating case which has the advantage that the y-dependence need not be considered. The equations are as above but with v = o, y = o and with y-derivatives ignored. The family of westward-propagating planetary waves is replaced by just two westward-propagating gravity modes, and this simplifies the mathematics considerably.

3. Normal modes

When ϕ is constant, i.e. both layers are of constant depth, it is useful to express the motion in terms of normal modes (Gill 1982a, Chapter 6). If λ times the second of (2.10) is added to the first of (2.10) it becomes

$$\frac{\partial H}{\partial t} + \frac{\partial U}{\partial x} + \frac{\partial V}{\partial y} = 0 \quad (3.1)$$

where

$$\left.\begin{aligned} H &= h_1 + \lambda h_2 \\ U &= \phi u_1 + \lambda(1-\phi)u_2 \\ V &= \phi v_1 + \lambda(1-\phi)v_2 \end{aligned}\right\} \quad (3.2)$$

Similarly ϕ times (2.9) with index i = 1 plus λ ($1-\phi$) times (2.9) with i = 2 results in

$$\left.\begin{aligned} \frac{\partial U}{\partial t} - \tfrac{1}{2} y V &= -c^2 \frac{\partial H}{\partial x} \\ \frac{\partial V}{\partial t} + \tfrac{1}{2} y U &= -c^2 \frac{\partial H}{\partial y} \end{aligned}\right\} \quad (3.3)$$

provided that c^2 and λ satisfy

$$c^2 = \phi + r(1-\phi)\lambda = r(1-\phi) + r\phi/\lambda . \quad (3.4)$$

The last equation gives a quadratic for λ, namely

$$r(1-\phi)\lambda^2 + (\phi - r + r\phi)\lambda - r\phi = 0 \quad (3.5)$$

and so

$$2r(1-\phi)\lambda = r - \phi - r\phi \pm S \quad (3.6)$$

$$2c^2 = r + \phi - r\phi \pm S \quad (3.7)$$

where

$$\left.\begin{aligned} S^2 &= (r - \phi - r\phi)^2 + 4r^2\phi(1-\phi) \\ &= (r + \phi - r\phi)^2 - 4r(1-r)\phi(1-\phi) \end{aligned}\right\} \quad (3.8)$$

For the model studied here, r is given the value 0.5 so that the change of density at the two interfaces is the same. The value of ϕ is 0.5 to the west of the shoaling region, so the incident wave comes from a region where the two layers are of equal thickness. In this region

$\lambda = 0.6180$, $c = 0.8090$ (1st mode)

or $\lambda = -1.6180$, $c = 0.3090$ (2nd mode) .

The value of ϕ reduces to a small value in the shoaling region. For small ϕ, neglecting terms of order ϕ^2 relative to the leading order terms

$\lambda \approx 1-\phi$, $c \approx 0.7071$ (1st mode)

$\lambda \approx -\phi(1+2\phi)$, $c \approx 0.7071\,\phi^{1/2}(1 - 1/2\phi)$ (2nd mode).

In this limit, the first mode behaves as if the uppermost layer did not exist and the wave speed is $(g_2(H_1+H_2))^{1/2}$. The second mode behaves as if the second layer is infinitely deep and therefore inactive, the wave speed being $(g_1 H_1)^{1/2}$.

4. Energy analysis

It is helpful to analyse the solutions to the shoaling thermocline problem in terms of the zonal energy flux. An energy equation can be derived by taking

$$\phi u_1 \times (2.9a, i=1) + \phi v_1 \times (2.9b, i=1)$$
$$+ (1-\phi) u_2 \times (2.9a, i=2) + (1-\phi) v_2 \times (2.9b, i=2)$$
$$+ p_1 \times (2.10a) + p_2 \times (2.10b)$$

to give an equation of the form

$$\frac{\partial E}{\partial t} + \frac{\partial J}{\partial x} + \frac{\partial K}{\partial y} = 0 .$$

In this equation, the energy density is given by

$$E = \tfrac{1}{2}\phi u_1^2 + \tfrac{1}{2}\phi v_1^2 + \tfrac{1}{2}(1-\phi) u_2^2 + \tfrac{1}{2}(1-\phi) v_2^2 + \tfrac{1}{2} h_1 (h_1 + r h_2) + \tfrac{1}{2} h_2 (r h_1 + r h_2) \qquad (4.1)$$

and the local zonal energy flux by

$$J = (h_1 + r h_2)\phi u_1 + (r h_1 + r h_2)(1-\phi) u_2 . \qquad (4.2)$$

In a rotating model the total zonal energy flux across a meridian is $\int J\,dy$, while in a non-rotating model the form given in (4.2) can be used as it stands. For the non-rotating model the formula for E given in (4.1) needs to be modified by excluding the terms involving v.

It would be possible to obtain a variety of different expressions for E and J by adding a constant to p_i in equations (2.11): this is equivalent to changing the reference level for potential energy. However (4.1) and (4.2) give the unique expressions for E and J in

which all terms are quadratic in the perturbation quantities. It is necessary to choose this form for the energy equation in order to establish certain orthogonality properties.

In the non-rotating case the four possible modes of disturbance are orthogonal to one another in the sense that the energy density and energy flux of a linear combination of modes is equal to the same linear combination of the energy densities and flux of each mode. Proof of these orthogonality properties is given by King (1985).

One important consequence of these orthogonality properties is that since any disturbance can be uniquely decomposed into the sum of vertical modes, its energy can be uniquely and conservatively distributed between the vertical modes.

5. The high-frequency limit

The geometry of the problem is shown in Fig. 1. An incident wave of wavenumber k and frequency w impinges on the shoaling thermocline from the west. The shoaling section lasts for a distance D. the problem is to find what waves are transmitted out of the shoaling region into the uniform region to the east, and what wave energy is reflected back into the uniform region to the west. The parameters of the problem in the non-rotating case are the geometrical ones r, ϕ_o, ϕ_1, and kD, where ϕ_o and ϕ_1 are the values of ϕ in the uniform regions to the west and east, respectively, of the shoaling zone. In this paper, r and ϕ_o are given values of 0.5 and ϕ_1 is given a small value (typically 0.05), so the main parameter which can vary is kD. In the rotating case there is an extra parameter kR, where R is the Rossby radius. In this paper, however, the long-wave approximation is made i.e. kR and R/D are both assumed small. Thus the main variable parameter is still kD.

In this section the limiting case where

$$kD \gg 1 \qquad (5.1)$$

is considered, i.e. the wavelength is small compared with the length of the shoaling region and the frequency ω of the incident wave is large compared with c/D. Another way of expressing the same limit is to rescale x so the wavenumber of the incident wave is unity. Then the slope ϵ of the interface is very small and the wave changes only slowly with x. One can derive an equation for the amplitude of a given mode in the shoaling region, but this equation contains terms involving the other mode as the two modes are not independent. These extra terms include a factor ϵ as the modes are only weakly coupled.

The small ϵ limit can be determined using the equation as a starting point and carrying out a great deal of algebra. Rather than present this algebra, we choose to state the result, which accords with intuition, and refer the reader to King (1985) for details. This result is that a single mode incident on the shoaling region remains as the same mode throughout, changing its wave speed and its vertical profile slowly as it progresses. The changes in amplitude follow from the condition of constant eastward energy flux J.

To apply the result, consider first the non-rotating case where the solution of (3.1) and (3.3) for a single eastward-travelling mode in a region of uniform wave speed c has the form

$$\left.\begin{aligned} H &= F\left(\tfrac{x}{c} - \epsilon\right) \\ U &= c\,F\left(\tfrac{x}{c} - \epsilon\right) \end{aligned}\right\} \qquad (5.2)$$

where F is an arbitrary function. For the wave impinging on the shoaling region from the west, this function is known. When the wave enters the shoaling region where c varies, the wave is modified to

take the form

$$\left.\begin{aligned} H &= A(x)\, F\left(\int \frac{dx}{c} - t\right) \\ U &= cA(x)\, F\left(\int \frac{dx}{c} - t\right) \end{aligned}\right\} \quad (5.3)$$

where, for any given time, A varies much more slowly with x than F does. F is a known function and A needs to be determined from the condition of constant flux J. The coefficient A is defined to be unity for the incident signal. To apply this, the quantities u_i, h_i in (4.1) need to be related to U, H for the case where all the energy is in one mode.

Suppose that the variables H, U and the parameter λ in (3.2) refer to the mode in question, whereas λ' refers to the other mode which has zero amplitude. Thus (3.2) requires

$$h_1 = -\lambda' h_2 \qquad \phi u_1 = -\lambda'(1-\phi) u_2 \,. \quad (5.4)$$

The root λ' of (3.5) can be related to the root λ by virtue of their product satisfying the standard relation for a quadratic, which in this case gives

$$\lambda\lambda' = -\phi/(1-\phi) \quad (5.5)$$

Thus (5.4) can be rewritten as

$$(1-\phi)\,\lambda h_1 = \phi h_2 \qquad \lambda u_1 = u_2 \quad (5.6)$$

Substituting in (3.2) then gives

$$\left.\begin{aligned} h_1 &= \phi H/B & h_2 &= (1-\phi)\lambda H/B \\ u_1 &= U/B & u_2 &= \lambda U/B \\ \text{where} \quad B &= \phi + (1-\phi)\lambda^2 \,. \end{aligned}\right\} \quad (5.7)$$

These can now be substituted in the expression (4.2) for J, and (3.5) can be used to put ϕ in terms of λ to yield

$$J = \frac{r(1-r)}{\lambda^2 - 2r\lambda + r} HU \quad . \qquad (5.8)$$

From (5.3), therefore, constancy of J requires

$$\frac{r(1-r)\, c\, A^2}{\lambda^2 - 2r\lambda + r} = \text{constant} \qquad (5.9)$$

where the constant is determined from the wave properties before the wave enters the shoaling region. For the standard case where r = 1/2 and ϕ = 1/2 west of the shoaling region

$$\frac{c A^2}{\lambda^2 - \lambda + \frac{1}{2}} = \begin{cases} 3.0652 & \text{for mode 1} \\ 0.0652 & \text{for mode 2.} \end{cases}$$

Figure 2 shows the way c, λ and A vary with ϕ for this case, both for mode 1 (Fig. 2a) and mode 2 (Fig. 2b). For small ϕ the asymptotic results are

$$A \approx 1.4722(1-\phi) \quad \text{for mode 1}$$

$$A \approx 0.2148\, \phi^{-1/4}(1+1.25\phi) \quad \text{for mode 2.}$$

The results are easily generalised to the case of equatorial Kelvin waves because the solutions for H and U are then identical to (5.2) and (5.3) apart from a multiplying factor which, in dimensional terms, has the form

$$\exp(-\beta y^2/2c) \quad .$$

The condition of constant eastward energy flux becomes $\int J\,dy$ is equal to a constant, so that (5.9) is altered by an additional factor $c^{1/2}$ on the left hand side. The way A varies with ϕ in the equatorial case is also shown in Fig. 2, and differs rather little from the non-rotating case.

6. The low-frequency limit

For a wave of very low frequency, i.e. of very long wavelength, the shoaling region appears to be so short that it is equivalent asymptotically to a step where ϕ changes suddenly from its western value ϕ_0 to its eastern value ϕ_1, at x = 0. Solution of this limiting problem in the non-rotating case is quite straightforward.

An incident signal (specified, and propagating eastwards) can give rise to a transmitted and a reflected signal. Each signal can be a combination of the two modes and so there are four amplitudes to be determined. There are also four jump conditions which are:-

continuity of the mass fluxes ϕu_1 and $(1-\phi)u_2$

and

continuity of the perturbation pressures h_1 and h_2.

It follows further from those conditions that the zonal energy flux is continuous. We will use subscripts 1 and 2 to denote modes 1 and 2 and subscripts l and r to denote quantities to the left or right of the step, which is taken to be at x = 0. We use $c_{1l}, c_{2l}, c_{1r}, c_{2r}$ to denote the (positive) speeds of the relevant modes.

For i = 1,2, I_i, R_i, T_i denote the amplitudes of the incident, reflected and transmitted signals respectively. To the left of the step,

$$\left.\begin{aligned}
H_{1l} &= I_1 \exp\left(-i\omega\left(t-\tfrac{x}{c_{1l}}\right)\right) + R_1 \exp\left(-i\omega\left(t+\tfrac{x}{c_{1l}}\right)\right)\\
U_{1l} &= c_{1l} I_1 \exp\left(-i\omega\left(t-\tfrac{x}{c_{1l}}\right)\right) - c_{1l} R_1 \exp\left(-i\omega\left(t+\tfrac{x}{c_{1l}}\right)\right)\\
H_{2l} &= I_2 \exp\left(-i\omega\left(t-\tfrac{x}{c_{1l}}\right)\right) + R_2 \exp\left(-i\omega\left(t+\tfrac{x}{c_{2l}}\right)\right)\\
U_{2l} &= c_{2l} I_2 \exp\left(-i\omega\left(t-\tfrac{x}{c_{2l}}\right)\right) - c_{2l} R_2 \exp\left(-i\omega\left(t+\tfrac{x}{c_{2r}}\right)\right)
\end{aligned}\right\} \quad (6.1)$$

and to the right of the step

$$\left.\begin{aligned} H_{1r} &= T_1 \exp\left(-i\omega\left(t-\tfrac{x}{c_{1r}}\right)\right) \\ U_{2r} &= c_{1r} T_1 \exp\left(-i\omega\left(t-\tfrac{x}{c_{1r}}\right)\right) \\ H_{2r} &= T_2 \exp\left(-i\omega\left(t-\tfrac{x}{c_{2r}}\right)\right) \\ U_{2r} &= c_{2r} T_2 \exp\left(-i\omega\left(t-\tfrac{x}{c_{2r}}\right)\right) . \end{aligned}\right\} \quad (6.2)$$

The quantities which are continuous at the step are related to the mode amplitudes by

$$\left.\begin{aligned} h_1 &= (\lambda_2 H_1 - \lambda_1 H_2)/(\lambda_2 - \lambda_1) \\ h_2 &= (H_2 - H_1)/(\lambda_2 - \lambda_1) \\ \phi u_1 &= (\lambda_2 U_1 - \lambda_1 U_2)/(\lambda_2 - \lambda_1) \\ (1-\phi) u_2 &= (U_2 - U_1)/(\lambda_2 - \lambda_1) . \end{aligned}\right\} \quad (6.3)$$

Enforcing continuity of those quantities at x = 0 gives

$$\left.\begin{aligned} \lambda_{2\ell}(I_1+R_1) - \lambda_{1\ell}(I_2+R_2) &= (\lambda_{2r} T_1 - \lambda_{1r} T_2)\alpha \\ (I_2+R_2) - (I_1+R_1) &= (T_2 - T_1)\alpha \\ \lambda_{2\ell} c_{1\ell}(I_1-R_1) - \lambda_{1\ell} c_{2\ell}(I_2-R_2) &= (\lambda_{2r} c_{1r} T_1 - \lambda_{1r} c_{2r} T_2)\alpha \\ c_{2\ell}(I_2-R_2) - c_{1\ell}(I_1-R_1) &= (c_{2r} T_2 - c_{1r} T_1)\alpha \end{aligned}\right\} \quad (6.4)$$

where the ratio α is given by

$$\alpha = \frac{\lambda_{2\ell} - \lambda_{1\ell}}{\lambda_{2r} - \lambda_{1r}}$$

For any chosen values of I_1 and I_2, equations (6.4) may be solved to give values of R_1, R_2, T_1, and T_2. These are the amplitudes of H in the reflected and transmitted signals. The values of u_1, u_2, h_1, h_2 are then given by (5.9) with λ, ϕ and c taking appropriate values for each mode and each side of the step. Note that $c < 0$ for the reflected signals.

It is convenient to define the incident signal in terms of the proportion of incident energy in each mode. This however contains some ambiguity because J is quadratic in H ; specifying a certain amount of energy to be incident in mode 1 determines the magnitude of I_1 but not the sign. This is important when the incident signal is a mixture of modes 1 and 2.

The results of solving (6.4) are illustrated in Figs. 3 and 4. For all cases it is assumed that r = 0.5 throughout the basin and that $\phi_0 = 0.5$.

Figure 3 shows how the incident energy is split between T_1 , T_2 and $R_1 + R_2$ as ϕ_1 varies and for a variety of incident energy distributions. The split of incident energy between I_1 and I_2 is the same as the split between T_1 and T_2 when = 0.5 (i.e. there is no step). Panels (a) and (b) correspond to the incident signal having just one mode and panels (c) to (h) correspond to mixed mode cases. Notice that for any choice of how the incident energy is to be split between two modes, there are two quite different solutions depending on whether $I_1 I_2$ is positive ((c) to (e)) or negative ((f) to (h)). The reason for this difference is that depending on the sign of $I_1 I_2$, the energy converted from mode 2 to mode 1 (for example) will be added to or subtracted from the energy incident as mode 1 and transmitted as mode 1.

It can further be seen from Fig. 3 that except in cases of very severe jumps, relatively little energy is reflected. In each panel, the minimum value of ϕ_1 is 0.01 which corresponds to a reduction of the thermocline depth by 98% For ϕ_1= 0.05, the maximum proportion of incident energy that is reflected is 25%.

In Fig. 4, ϕ_1 is fixed at 0.05 and the proportion of incident energy in mode 1 varies between 0 and 100%. Again there are two solutions depending on whether $I_1 I_2$ is positive (4(a)) or negative (4(b)). In panels (a) and (b) the lowest region is the proportion of incident energy transmitted as mode 1 (measured on the left hand scale) and the upper region is the proportion transmitted as mode 2 (measured on the right hand scale). The middle region is the proportion of incident energy that is reflected. Since we are particularly interested in the signal on the right hand side of the step, the distribution of transmitted energy (which for $\phi = 0.05$ is a minimum of 75% of incident energy) between modes 1 and 2 is given in Fig. 4(c). The two branches of the curve (solid and broken) correspond to different signs of $I_1 I_2$. It is interesting to observe that when the incident signal is mixed with 50% energy in each mode, the transmitted signal has 90% energy in one or other mode. Notice too how steep the the curves are when the incident energy has a small proportion in one or other mode. When I_1 has 80% of incident energy, T_2 can have more than 70% or less than 5% of transmitted energy; thus the distribution of transmitted energy can be very sensitive to small variations in the distribution of incident energy. However, it is quite possible that a predominantly mode 1 incident signal can give rise to a predominantly mode 2 transmitted signal.

The low-frequency limiting solution in the rotating case could similarly be studied by applying matching conditions at a step, but the problem is considerably more complicated because functions of latitude need to be matched (not just amplitudes) and there is an infinite set of possible wave modes to consider. This problem is not solved here for that reason, but it will be found that the results for the non-rotating case provide a useful background for the results

found computationally for the rotating case.

The conclusions from the studies of the two limits of high-frequency or low-frequency incident signals are that in the high-frequency case energy is not exchanged between modes but in the low-frequency case considerable energy can be transferred. The question now arises of how much energy is transferred in intermediate cases.

7. Numerical solutions for incident Kelvin waves

The problem of incident Kelvin waves on a shoaling thermocline was solved numerically using a model developed by King (1985). This is a two-layer model which can solve (2.9) and (2.10) or their non-linear equivalents. It is computationally very efficient because it makes the low-frequency or long-wave approximation which excludes the acceleration term $\partial v_i/\partial t$ from (2.9b). The dynamical consequence of this is that planetary waves are made non-dispensive and the short eastward-propagating planetary waves are excluded (Gill, 1982a). As to the problem tackled here, it means that the waves considered in Section 5 which are short compared with the length of the shoaling region are still considered long relative to the Rossby radius.

In the numerical experiments, a single Kelvin wave pulse of total zonal length L and with sloping leading and trailing edges, is "fired" at the region, with zonal length D, in which ϕ reduces from 0.5 to 0.05 (i.e. the fraction of the active layers occupied by the uppermost layers reduces from a half to one twentieth). The ratio L/D is the only parameter which is changed from experiment to experiment. It ranges from small values where the WKBJ approximation is applicable to large values where the shoaling region would be expected to behave like a step.

The results are shown in Fig. 5, where the value at the equator of the energy flux J for the second mode transmitted pulse is given as a percentage of the value at the equator for the incident first mode pulse.

As expected from WKBJ theory, very little second mode response is found for small L/D, but the response increases as L/D increases. For large L/D, the non-rotating case (Fig. 4) gives about a quarter of the

transmitted energy in mode 2, and the equivalent value is shown in Fig. 5. In the rotating case, the numerical results show that the mode-2 transmitted flux at the equator is 34% of the incident value at the equator. On the other hand, if the total flux is found by integrating J with respect to latitude, the equatorial values need to be multiplied by $c^{1/2}$ and so the percentage of the incident flux found transmitted in mode 2 is 15%.

Perhaps the most useful aspect of Fig. 5 is that it shows the range of values of L/D over which the transition from the WKBJ to the step limit take place. From the figure, the intermediate values of L/D are between 1.5 and 3 so if D is 60° of longitude, the transition wavelengths, as measured by 2L, are between 180° and 360°. For a first mode propagating at about 60° per month this corresponds to periods of 3 to 6 months. Thus the energetic 2 to 3 week waves are in the WKBJ range and an incident first mode wave will remain a first mode wave. On the other hand, pulses of more than 50 days' duration (i.e. L/D > 1.5), like the ones associated with El Nino, will be significantly distorted by the shoaling thermocline.

The way energy is transferred between modes over the shoaling zone is shown for a mid-transition case (L/D=1.4) in Fig. 6 where mode 1 and mode 2 amplitudes are given as functions of longitude and time. The shoaling region extends from longitude 0° to 60°. It can be seen that the energy transfer occurs gradually over the shoaling region so that the two waves have already started to separate at the end of the shoaling region. It is also interesting to see what these results mean in terms of values of u_1 and u_2 at the equator. If $u_1 = 1$ and $u_2 = .62$ for the incident pulse, one sees two peaks in u_2 at the end of the shoaling zone (60° longitude). The first peak has $u_1 = 0.99$, $u_2 = 0.89$ where the first mode dominates, and the

second one has $u_1 = 2.65$, $u_2 = -0.23$ where the second mode dominates. The corresponding figures for h_1 and h_2 are 0.62, 0.38 for the incident wave, 0.08, 1.15 for the first peak and 0.82, - 0.96 for the second peak.

For comparison, the results for the case L/D=4.2 which is close to the step limit are also given. These are (u_1, u_2) = (1.0, 0.62) for the incident wave, (1.05, 0.82) for the first peak and (4.88, 0.48) for the second peak, and (h_1, h_2) = (0.62, 0.38) for the incident wave, (0.11, 1.04) for the first peak and (1.58, -1.76) for the second peak.

Fig. 6 also shows maps of mode 1 and mode 2 amplitude at two times. In the first picture, the mode 1 pulse has left the shoaling zone completely, but the mode 2 pulse has not yet fully emerged. At the second time the mode 1 pulse is not visible in the picture. The second mode, on the other hand, shows the Kelvin wave has emerged from the shoaling zone and a weak reflected planetary wave is also visible.

8. Conclusions

The implications of this study for the tropical Pacific Ocean are as follows. The energetic first mode Kelvin waves with periods of 2 to 3 weeks propagate along the equatorial wave guide with little transfer of energy to the second mode. As they propagate, however, the wave properties will change slowly because the structure of a mode 1 wave changes as the thermocline shoals. In particular, the wave speed decreases, the meridional scale decreases and the velocity becomes more uniform with depth in the upper layers ($\lambda \to 1$). The same should be true for all mode 1 waves with periods less than 3 months.

For longer periods, significant transfer does take place. For these long periods, it is perhaps more appropriate to think in terms of pulses during which the perturbation is of one sign, as appears to happen during El Nino events. The pulse duration can be regarded as equivalent to half a period of a wavelike signal. If the pulse duration is more than $1\frac{1}{2}$ months, significant transfer to mode 2 takes place. As the duration increases so does the amount of transfer, but this levels off for pulse durations over 3 or 4 months, as seen in Fig. 5. Thus during El Nino events the structure of perturbations in the eastern Pacific need not be dominated by the first baroclinic mode even if it is generated by an incident Kelvin wave which had predominantly first mode structure in the central Pacific.

References

Behringer, D.W., 1984: Equatorial modes in the eastern Pacific (85°W). J. Geophys. Res., 89, 3279-3731.

Behringer, D.W., 1985: Evidence for vertical modes during the 1982-83 El Nino. J. Phys. Oceanogr., to appear.

Eriksen, C.C., M.B. Blumenthal, S.P. Hayes, and P. Ripa, 1983: Wind generated equatorial Kelvin waves observed across the Pacific Ocean. J. Phys. Oceanogr., 13, 1622-1640.

Gent, P.R., 1985: The annual cycle in the central equatorial Pacific Ocean. J. Phys. Oceanogr., to appear.

Gill, A.E., 1982a: Atmosphere Ocean Dynamics. Academic press, 662 pp.

Gill, A.E., 1982b: Changes in thermal structure of the equatorial Pacific during the 1972 El Nino as revealed by bathythermograph observations. J. Phys. Oceanogr., 12, 1373-1387.

King, B.A., 1985: Low-frequency waves in equatorial oceans. Ph.D. dissertation, University of Cambridge.

Knox, R.A. and D. Halpbern, 1982: Long range Kelvin wave propagation of transport variations in Pacific Ocean equatorial currents. J. Mar. Res. 40 (supplement), 329-339.

Leetma, A., 1985: The vertical structure of events in the eastern Pacific: June 1981 to June 1984. J. Phys. Oceanogr., to appear.

Figure Captions

Fig. 1 Geometry of the problem. There are two active layers of undisturbed depths $H_1(x)$ and $H_2(x)$ as shown, the total depth H_1+H_2 being constant. There is an infinitely deep inactive layer below in which the motion is negligible. The interface between the two active layers is at a fixed depth for a semi-infinite region to the left of the diagram, and also has a fixed depth for a semi-infinite region to the right. The shoaling section is confined to a finite distance D.

Fig. 2 Variation with the depth ratio ϕ of the parameters λ and c and of the amplitude A (both for the rotating (broken line) and non-rotating (solid line) cases). (a) corresponds to mode 1 and (b) to mode 2.

Fig. 3 Percentage of the incident energy flux which appears in the mode 1 transmitted wave (T_1), the mode 2 transmitted wave (T_2) and as reflected waves (R_1+R_2) for the non-rotating case of a wave incident on a step. The layer depth ratio ϕ is 0.5 to the left of the step and has the value ϕ_1 to the right of the step. The incident conditions for the cases shown are (a) pure mode 2 and (b) pure mode 1. In cases (c) to (e) the percentage of incident mode 1 energy flux is 25%, 50% and 75% respectively with I_1 and I_2 having the same sign. Cases (f) to (h) are the same except that I_1 and I_2 have opposite signs.

Fig. 4 Transmision and reflection coefficients for the non-rotating case of a wave incident on a step when the layer depth ratio is 0.5 on the left (where the wave is incident) and 0.05 on the right (where the wave is transmitted). In (a), the subdivision of energy flux between modes in the incident wave is given on the horizontal axis, and the subdivision between transmitted mode 1 (T_1), transmitted mode 2 (T_2) and reflected modes (R_1+R_2) is shown on the vertical axis. In this case I_1 and I_2 have the same sign. (b) is the same except that I_1 and I_2 have opposite signs. In (c), the horizontal axis is as before, but the vertical axis shows only the subdivision of transmitted energy flux between the modes. The solid line corresponds to (a) and the broken line to (b).

Fig. 5 Percentage of incident energy flux, as measured at the equator, which is transmitted in mode 2 for the rotating case when the incident pulse is a pure mode 1 Kelvin wave. The ordinate is the logarithm (base 10) of the ratio of incident pulse length L to the zonal distance D over which shoaling takes place. The pulse has constant strength over the middle third of its length and builds up or falls off linearly to this value in the remaining thirds. The layer depth ratio is 0.5 west of the shoaling region and 0.05 to the east.

Fig. 6 (a) Longitude-time plots of first and second mode amplitudes for the case of an incident pure mode 1 Kelvin wave when L/D=1.4. The shoaling region extends from longitude 0° to 60°. Time is

shown in days and the first mode wave speed is 2° /day.

(b) Map of first and second mode amplitudes at time t = 84 days.

(c) Ditto, but at t = 125 days.

Fig. 1

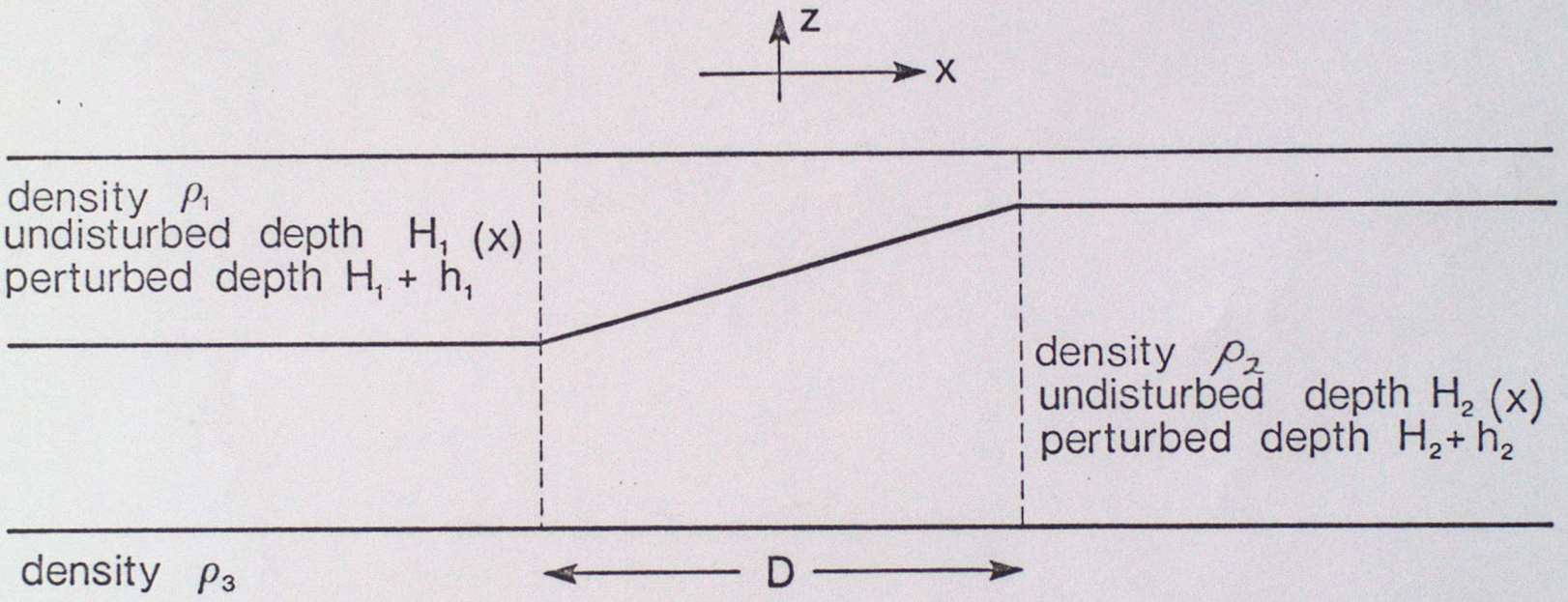
z
x
density ρ_1
undisturbed depth H_1 (x)
perturbed depth $H_1 + h_1$
density ρ_2
undisturbed depth H_2 (x)
perturbed depth $H_2 + h_2$
density ρ_3
D

30

Fig. 2

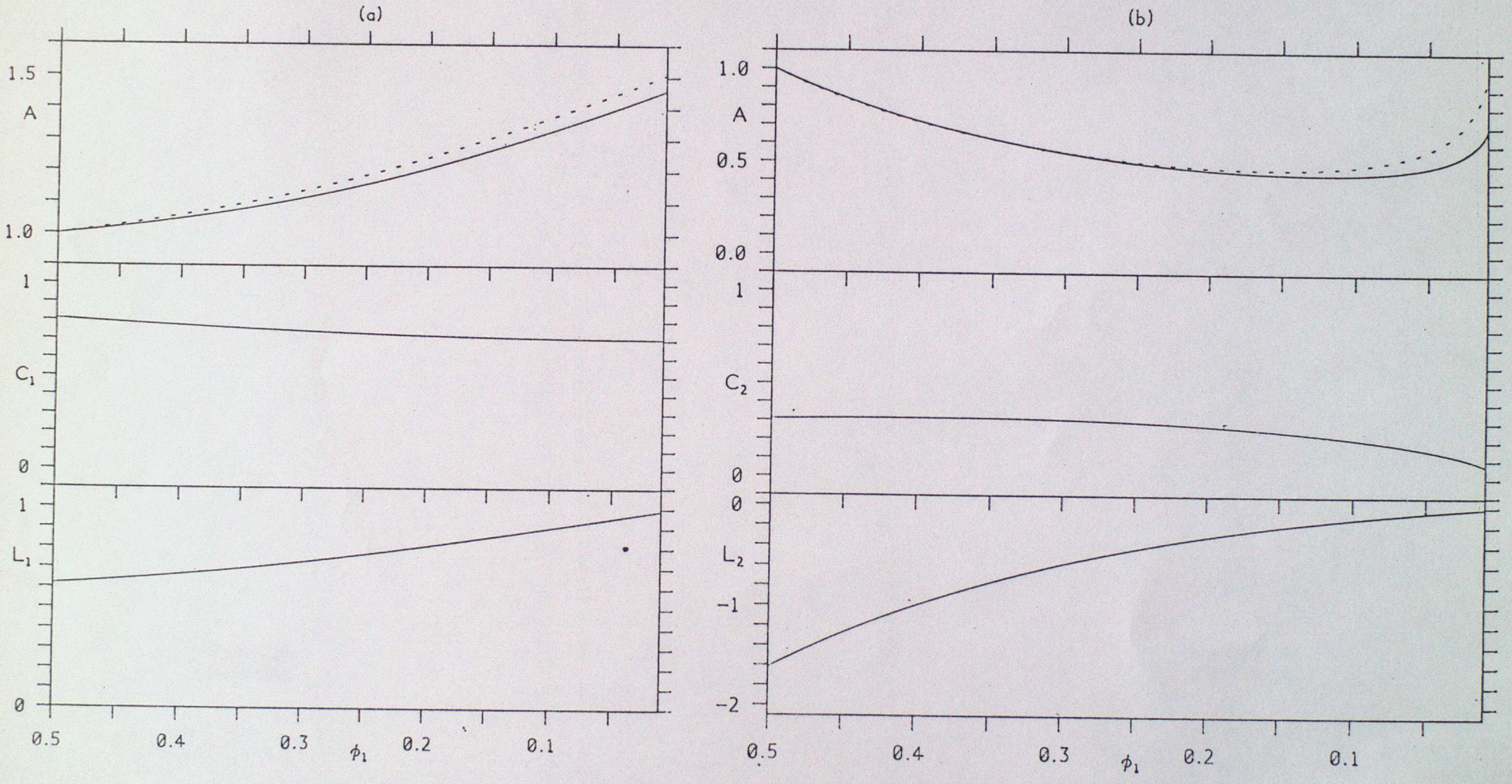
(a)
1.5
A
1.0
1
C_1
0
1
L_1
0
0.5
0.4
0.3
ϕ_1
0.2
0.1
(b)
1.0
A
0.5
0.0
1
C_2
0
0
L_2
−1
−2
0.5
0.4
0.3
ϕ_1
0.2
0.1

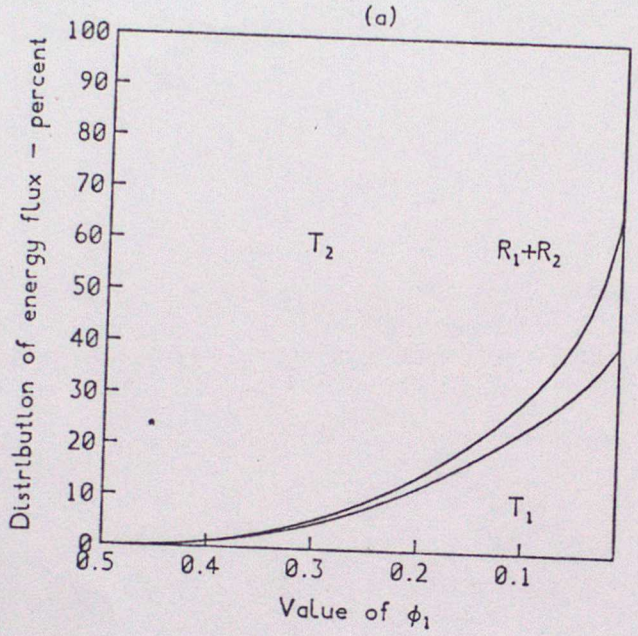
(a)
Distribution of energy flux – percent
100
90
80
70
60
50
40
30
20
10
0
T_2
R_1+R_2
T_1
0.5
0.4
0.3
0.2
0.1
Value of ϕ_1

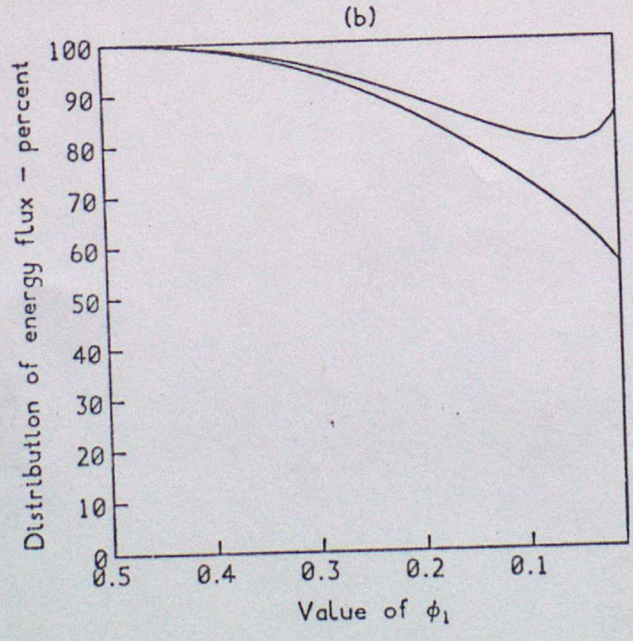
(b)
Distribution of energy flux – percent
100
90
80
70
60
50
40
30
20
10
0
0.5
0.4
0.3
0.2
0.1
Value of ϕ_1

Fig. 3

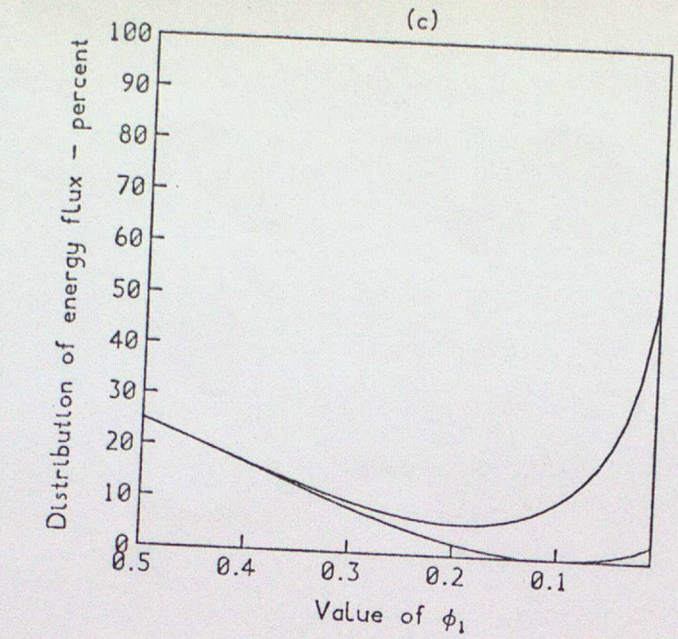
(c)
Distribution of energy flux – percent
100
90
80
70
60
50
40
30
20
10
0
0.5
0.4
0.3
0.2
0.1
Value of ϕ_1

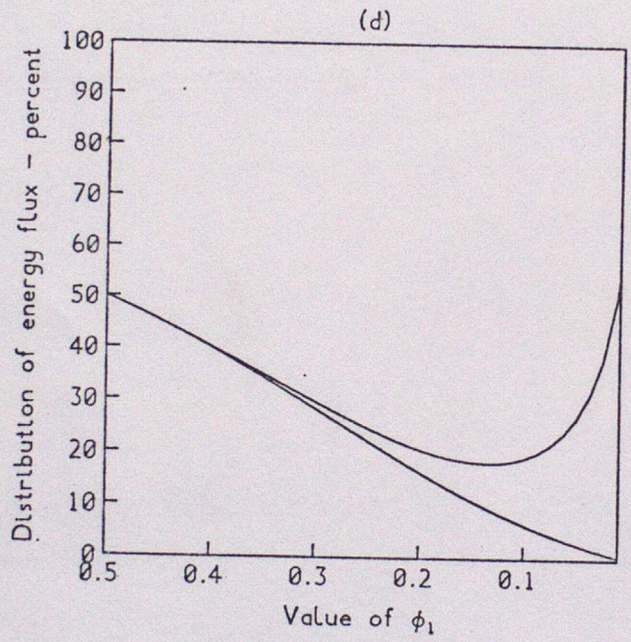
(d)
Distribution of energy flux – percent
100
90
80
70
60
50
40
30
20
10
0
0.5
0.4
0.3
0.2
0.1
Value of ϕ_1

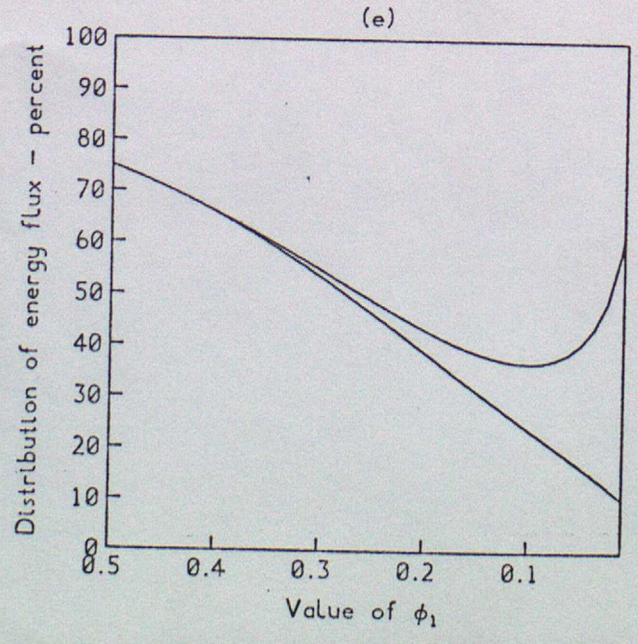
(e)
Distribution of energy flux – percent
100
90
80
70
60
50
40
30
20
10
0
0.5
0.4
0.3
0.2
0.1
Value of ϕ_1

Fig. 3

(f)

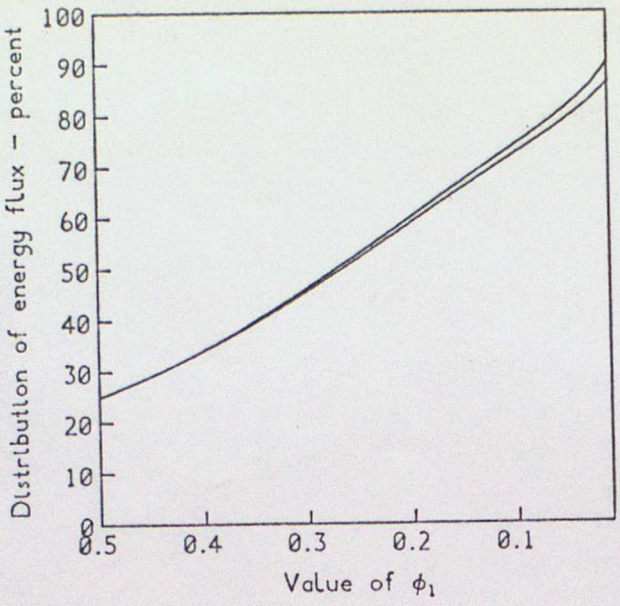
Distribution of energy flux - percent
100
90
80
70
60
50
40
30
20
10
0
0.5
0.4
0.3
0.2
0.1
Value of ϕ_1

(g)

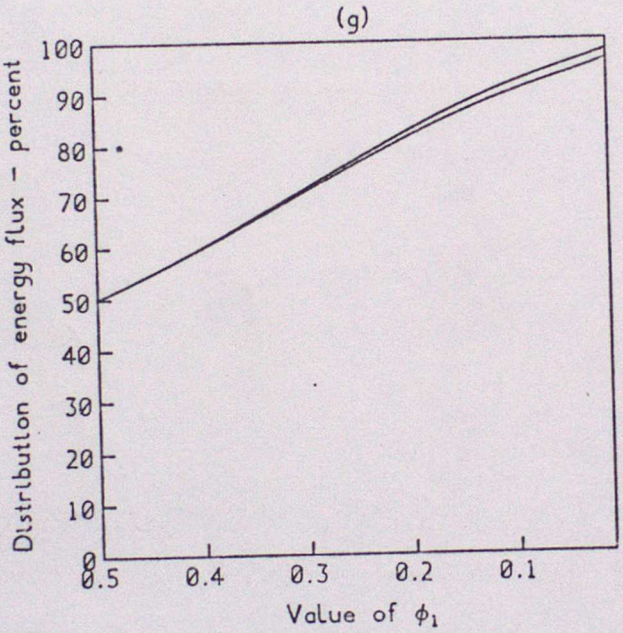
Distribution of energy flux - percent
100
90
80
70
60
50
40
30
20
10
0
0.5
0.4
0.3
0.2
0.1
Value of ϕ_1

Fig. 3

(h)

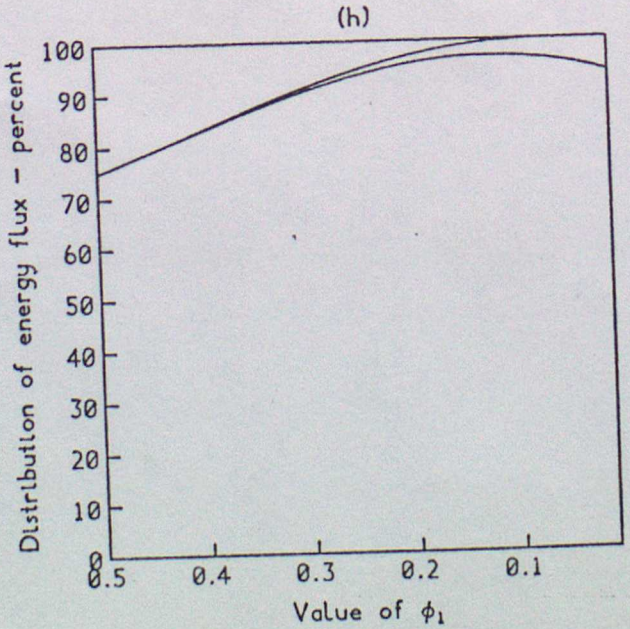
Distribution of energy flux - percent
100
90
80
70
60
50
40
30
20
10
0
0.5
0.4
0.3
0.2
0.1
Value of ϕ_1

(a)

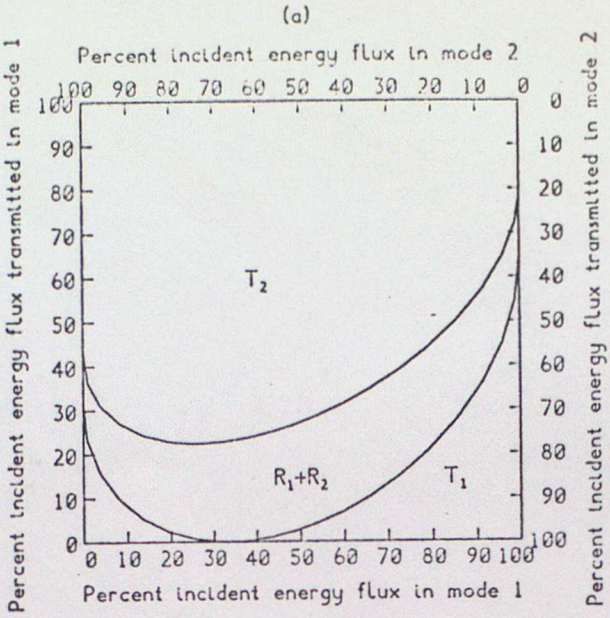
Percent incident energy flux in mode 2
Percent incident energy flux transmitted in mode 1
Percent incident energy flux transmitted in mode 2
Percent incident energy flux in mode 1
T2
R1+R2
T1

(b)

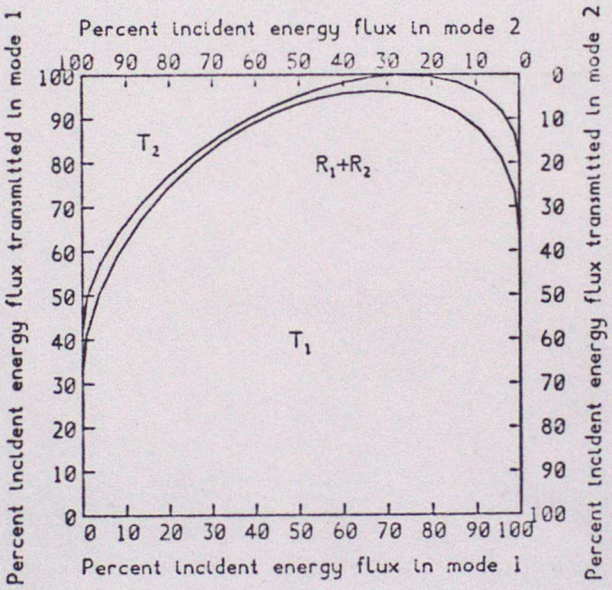
Percent incident energy flux in mode 2
Percent incident energy flux transmitted in mode 1
Percent incident energy flux transmitted in mode 2
Percent incident energy flux in mode 1
T2
R1+R2
T1

(c)

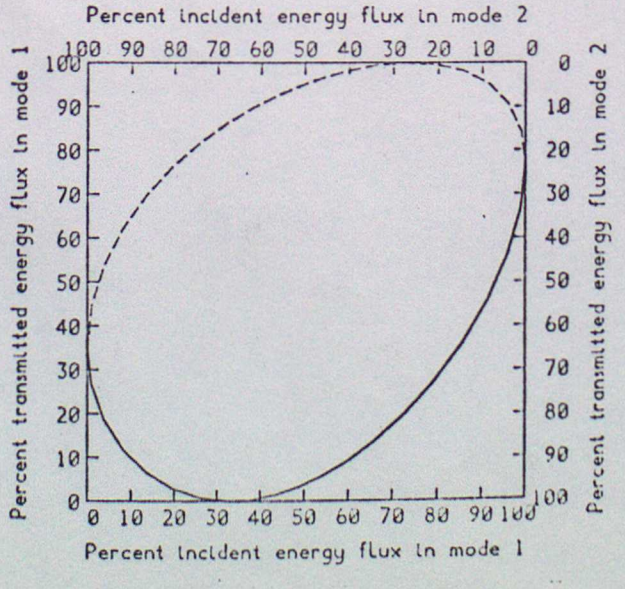
Percent incident energy flux in mode 2
Percent transmitted energy flux in mode 1
Percent transmitted energy flux in mode 2
Percent incident energy flux in mode 1

Fig. 4

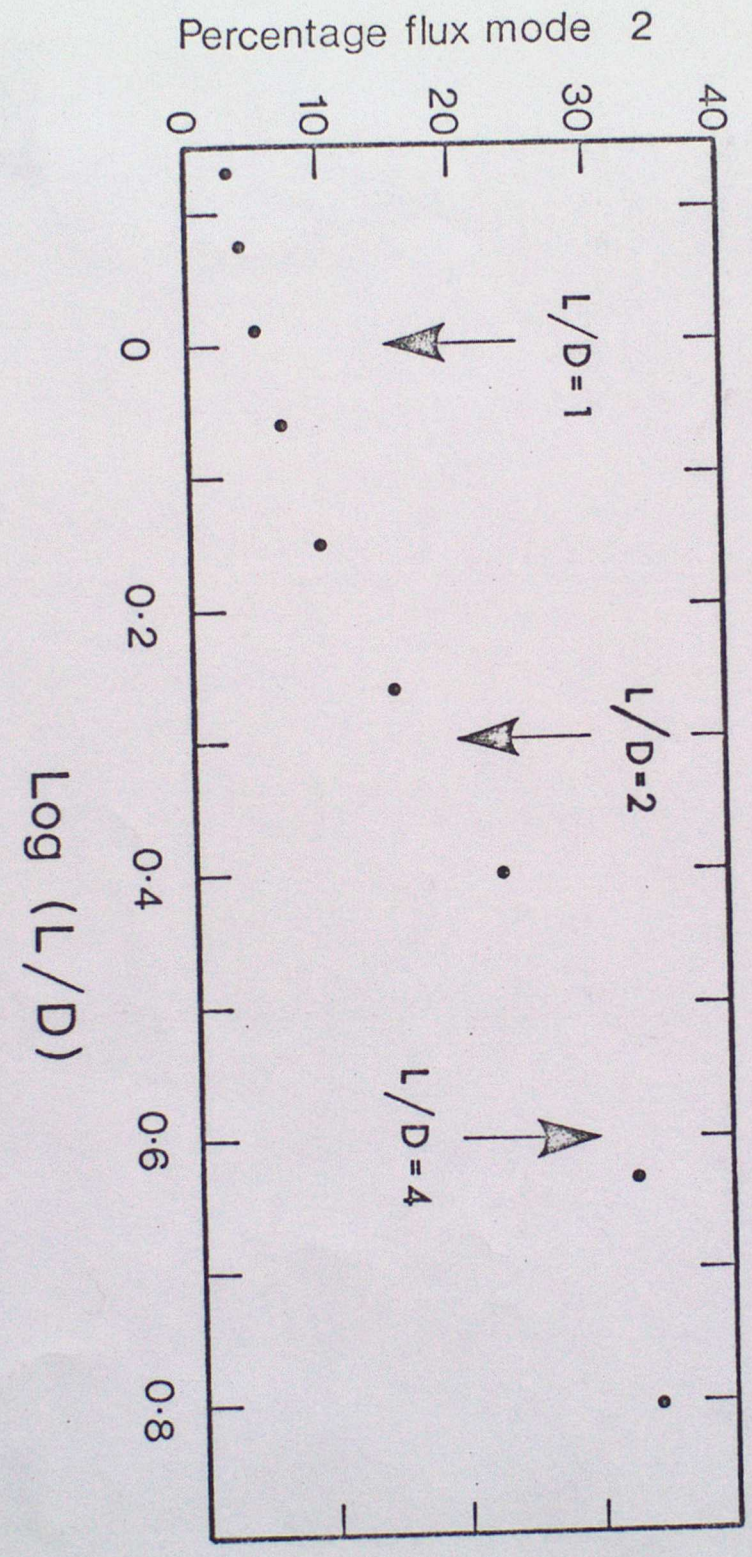
Percentage flux mode 2
0
10
20
30
40
0
0·2
0·4
0·6
0·8
Log (L/D)
L/D=1
L/D=2
L/D=4

Fig. 5

Fig. 6

(a)

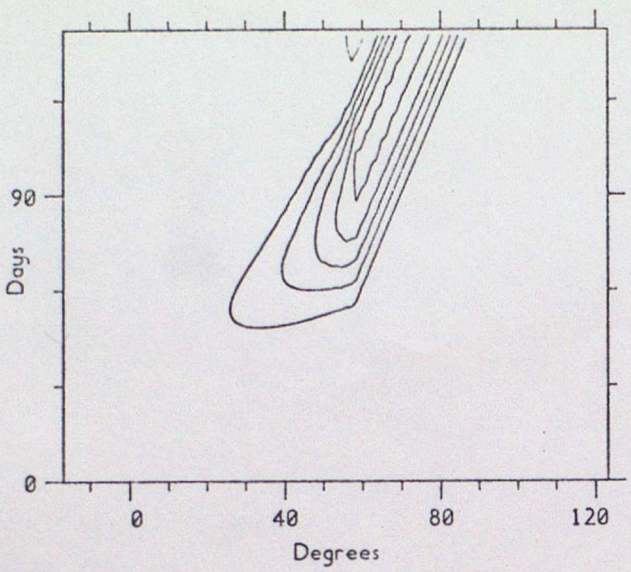

Mode 2 h anomaly

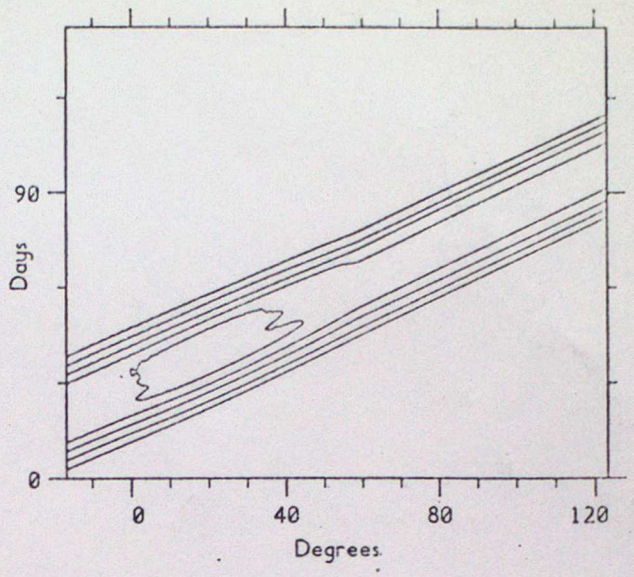

Linear

Mode 1 h anomaly

(b)

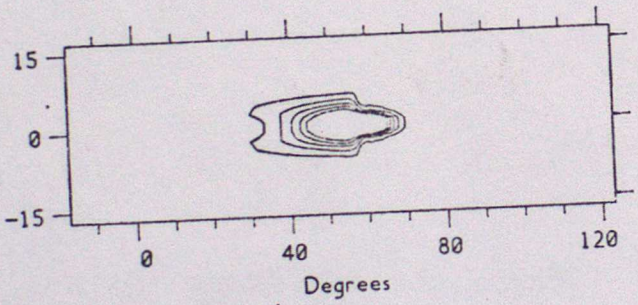

Mode 2 h anomaly

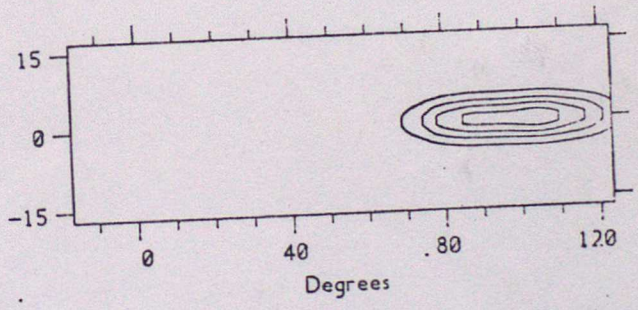

T = 83.6

Linear

Mode 1 h anomaly

(c)

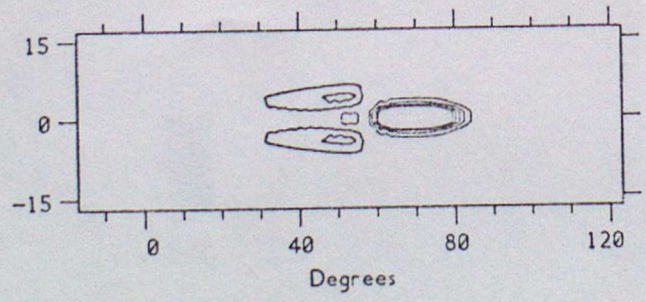

Mode 2 h anomaly

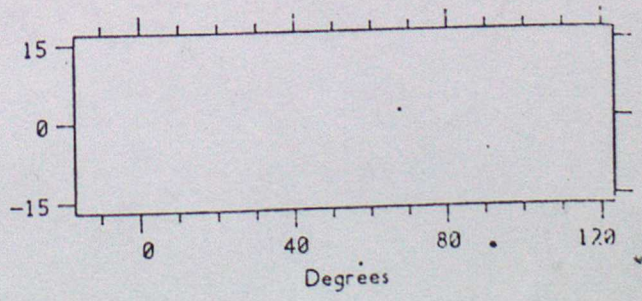

T = 125.4

Linear

Mode 1 h anomaly

DYNAMICAL CLIMATOLOGY TECHNICAL NOTES

DCTN 1	June 1984	A scheme for incorporating the thermodynamic sea-ice model into a coupled ocean-atmosphere model. C Gordon and M Bottomley
DCTN 2	Sept 1984	The parametrization of the upper ocean mixed layer in coupled ocean/atmosphere models. C Gordon and M Bottomley
DCTN 3	Sept 1984	The response of a simple thermodynamic sea-ice model to GCM forcing appropriate for perennial sea-ice. M Bottomley
DCTN 4	Sept 1984	Potential vorticity in the stratosphere derived using data from satellites. S A Clough, N S Grahame and A O'Neill
DCTN 5	Sept 1984	Simulation of the seasonal cycle of SST using globally specified climatological data to force simple ocean models. N S Grahame
DCTN 6	Sept 1984	Development of an improved GCM radiation scheme. A Slingo and R C Wilderspin
DCTN 7	Sept 1984	On the specification of surface fluxes in coupled atmosphere/ocean general circulation models. J F B Mitchell, C A Wilson and C M Price
DCTN 8	Sept 1984	A survey of possible repercussions of the Soviet river reversal programme on Arctic sea-ice. H Cattle
DCTN 9	Oct 1984	A study of a strong stratospheric warming during January 1982 T D A Fairlie
DCTN 10	Nov 1984	An intercomparison of the Met O 11 N45 model and the Met O 20 11-level model on the Cyber 205 J F Dyson
DCTN 11	Nov 1984	Simulation of observed time series of temperature and precipitation over eastern England. D N Reed
DCTN 12	Nov 1984	Forecasts and analyses of the onset of the Southwest monsoon. R Kershaw
DCTN 13	Nov 1984	On modelling the effects of CO_2 on climate. J F B Mitchell
DCTN 14	Dec 1984	Development of a revised longwave radiation scheme for an atmospheric general circulation model. A Slingo and R C Wilderspin
DCTN 15	Jan 1985	Rossby wavetrains in the stratosphere forced by localised disturbances in the troposphere. C J Marks (Oxford), A O'Neill and V D Pope

DYNAMICAL CLIMATOLOGY TECHNICAL NOTES

DCTN 16	Jan 1985	Observing system experiments using the Meteorological Office's 15-level model. R A Bromley
DCTN 17	Feb 1985	Atmospheric general circulation simulation of the climate of the Mediterranean region. H Cattle
DCTN 18	Feb 1985	Diurnal variation and cloud in a general circulation model. C A Wilson and J F B Mitchell
DCTN 19	Feb 1985	The sensitivity of the Saharan region in a general circulation model. W M Cunnington and P R Rowntree
DCTN 20	Mar 1985	The impact of aircraft observations on analyses and forecasts from the operational 15-level model. B R Barwell
DCTN 21	Mar 1985	Non-linear effects on heat-induced circulation of the tropical atmosphere. A E Gill and P J Phlips
DCTN 22	Apr 1985	Simulation of cloudiness with the U.K. Meteorological Office 11-layer AGCM. A Slingo and R C Wilderspin
DCTN 23	Apr 1985	An integrated approach to the representation of cloud processes. R N B Smith
DCTN 24	May 1985	Nuclear Winter: Calculations of the shortwave radiative effects of soot aerosols. A Slingo and P Goldsmith
DCTN 25	Jul 1985	Sea ice and the Antarctic winter circulation: a numerical experiment. J F B Mitchell and T S Hills
DCTN 26	Jul 1985	A Budyko-Sellers model for study of ocean-atmosphere interaction. W J Ingram
DCTN 27	Aug 1985	The effect of a shoaling thermocline on equatorially-trapped Kelvin waves. A E Gill and B A King